We are IntechOpen, the world's leading publisher of Open Access books Built by scientists, for scientists

4,800
Open access books available

122,000
International authors and editors

135M
Downloads

Our authors are among the

154
Countries delivered to

TOP 1%
most cited scientists

12.2%
Contributors from top 500 universities

CLARIVATE ANALYTICS BOOK CITATION INDEX INDEXED

WEB OF SCIENCE™

Selection of our books indexed in the Book Citation Index in Web of Science™ Core Collection (BKCI)

Interested in publishing with us?
Contact book.department@intechopen.com

Numbers displayed above are based on latest data collected.
For more information visit www.intechopen.com

Chapter

Harmonic Resonance Analysis for Wind Integrated Power System and Optimized Filter Design

Jignesh Pravinbhai Patel and Satish Kantilal Joshi

Abstract

As the contribution of renewable energy sources is increasing year over year, the effect of harmonics on power system becomes important, and it requires special attention. In conventional power sources, the harmonics is not generated at the source side; only load side is contributing in the harmonics. But renewable energy sources, particularly wind and solar, are based on power electronic devices, so it generates harmonics. This harmonics may have an adverse effect on the system. Harmonic resonance is one of the phenomena, due to which the harmonics are amplified and give rise to several trivial issues. Various methods are used to control the harmonics in the system. Harmonic filter is one of the simple ways to absorb the harmonics generated at load and generation side. Various filter designs have been found in literature as well as in the field. The filters are classified according to their design, construction and operation method. There are two main categories, active filters and passive filters. The passive filters are widely used due to its simplicity and lesser cost. However, to achieve the better performance, it is also used with active filters, and this combination is known as hybrid filter. The response of filters is modified as per the system requirement using various techniques. In this work, the impedance characteristics of various filters are discussed and analysed. Also, how the control structure of power electronic devices affects or modifies the output impedance of converter is also discussed.

Keywords: voltage source converter (VSC), pulse width modulation (PWM), grid-connected converter, filter, harmonic resonance, doubly fed induction generator (DFIG), Nyquist criteria, damped filter

1. Introduction

Voltage source converter (VSC) is widely used in industrial, commercial and renewable power generation applications. Out of many possible configurations, the three-phase and three-wire is widely used. During the last decade, the penetration of renewable energy sources has increased around the world. This is due to the increased concern worldwide about the carbon emission [1, 2]. The utilisation of energy from uncertain and variable sources has become possible with the use of these converters only.

For the purpose of this study, the analysis of VSCs is carried out assuming the ideal operating conditions of grid. But VSCs are never operating under such

conditions in practical. In a relatively weak system, VSCs are subject to various power quality disturbances, such as unbalance voltage, voltage swell and swag, notches, etc. [3]. The occurrence of such disturbances causes various problems like ripple in torque of generator and motor, increased losses, abnormal tripping of protective devices, malfunction of sophisticated control system, reduction in the expected lifetime of equipment, etc. [4].

There are two types of harmonics generated by VSCs. One is characteristics harmonics, which are related with the switching operations of the IGBTs inside the VSC. And second is non-characteristics harmonics. The voltage ripple on DC side of VSC generates harmonics on its AC side current. According to [5], the non-characteristics harmonics are generated by the unbalanced voltage in the AC side. However the quantification of magnitude of such harmonics is not simple and cannot be done with deterministic method. The non-characteristics harmonics are considered as the steady-state low-frequency components which would not appear if the grid voltage is balanced. The unbalance grid voltage has fundamental frequency negative sequence component and third-order positive sequence component.

Though it is possible to eliminate zero sequence third harmonic component using transformer of proper vector group, the non-characteristics third-order positive sequence harmonics cannot eliminate transformers with delta-connected winding.

In [6], the author has proposed DC voltage control to eliminate DC oscillating voltage when AC side is unbalanced. To achieve this, VSC has to operate with constant AC power control. However, the effect of control on AC current is not discussed. It is important to analyse the distorted and unbalanced AC side current, when such control is implemented. In this case, the currents of AC side of converter contain non-characteristics low-frequency component such as fundamental negative sequence and third harmonic components of positive and negative sequence.

2. Modelling of the voltage source converter

The total DC current I_{dc} is flowing to the DC side of VSC. V_{dc} is the instantaneous voltage across the capacitor, and id is the instantaneous DC current. The quality factor of DC capacitor is assumed to be high, so the series resistance is neglected. The instantaneous power is supplied by the renewable energy source, i.e. wind turbine. The instantaneous current I_s is supplied by the external source. It is equal to zero when VSC operates as a reactive power compensator.

The block diagram of VSC control structure is depicted in **Figure 1**. The control system consists of (i) voltage control, (ii) a phase lock loop (PLL), (iii) current reference calculation block and (iv) current control. The real power reference is

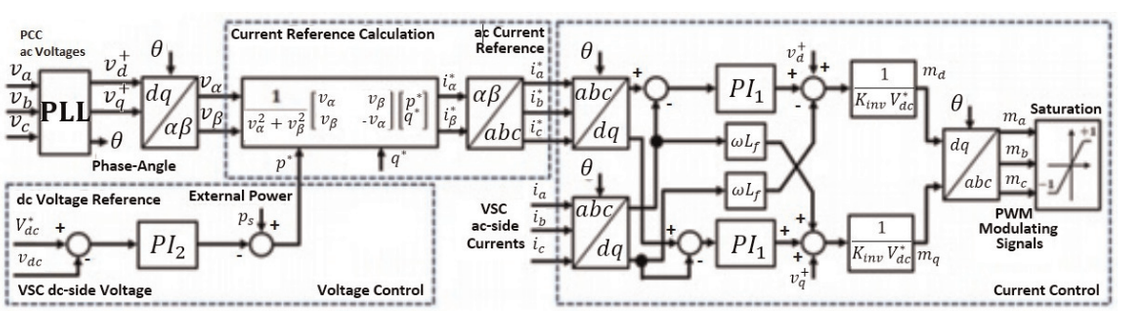

Figure 1.
Control structure of grid-connected wind converters.

calculated by the PI controller, which considers the DC voltage and desired active power through the VSC to the grid. The instantaneous reactive power is calculated by the separate loop, which may consider either the desired power factor or the reference voltage. The dq frame is synchronised with the positive sequence fundamental voltage of the grid at PCC with the help of PLL. It converts three phase voltages V_a, V_b and V_c into V_d+ and V_q+, which are converted in the alpha-beta reference frame voltages V_α and V_β. Then current reference is obtained by the α-β to *abc* transformation. These reference currents are compared with actual current, and modulating signals m_d and m_q are generated. These signals are finally transformed into m_a, m_b and m_c to generate pulse width modulated (PWM) signal.

Both switching frequency and grid voltage distortion can cause poor power quality. A filter design is a subject that requires trade-off between filter performance and the control bandwidth. Filters are required to meet power quality standard, avoid parallel resonance and improve power quality.

Inverter for grid interfacing will need to incorporate interface filters to attenuate the injection of current harmonics.

3. Impedance-based stability analysis

This method was proposed in [7]. The system impedance is partitioned into source and grid impedance. The source impedance is either represented by Thevenin's equivalent circuit or Norton equivalent circuit (**Figures 2** and **3**). Thevenin's equivalent circuit consists of ideal voltage source in series with the series impedance (Z_s), whereas the load impedance is modelled by series impedance (Z_l). Since the converter circuit is non-linear, it is represented by the small signal circuit. This linear representation of circuit is valid only for the small perturbation of signal. With this assumption, the current (I) flowing from source to load is given by

$$I(s) = \frac{V_s(s)}{Z_l(s) + Z_s(s)} \tag{1}$$

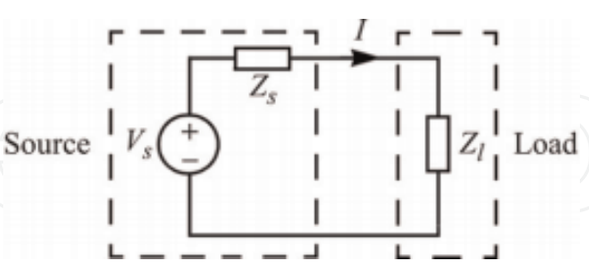

Figure 2.
Thevenin's equivalent circuit.

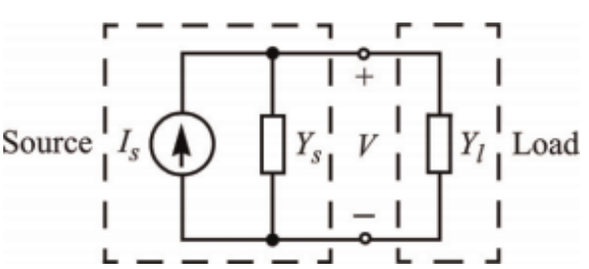

Figure 3.
Norton's equivalent circuit.

Which is rearranged as,

$$I(s) = \frac{V_s(s)}{Z_l(s)} \cdot \frac{1}{1 + {}^{Z_s(s)}\!/_{Z_l(s)}} \tag{2}$$

System stability analysis is based on the assumption that the source voltage and load impedance remain stable. So, *V(s)* and *1/Z(s)* are stable. So, the stability depends on the extreme right-hand side of Eq. (2). It is given by

$$H(s) = \frac{1}{1 + {}^{Z_s(s)}\!/_{Z_l(s)}} \tag{3}$$

The close observation of Eq. (3) reveals the important characteristics. It is a transfer function with unity gain and feedback equal to $Z_s(s)/Z_l(s)$. According to the linear control theory, the H(s) is stable, if and if only, when ration $Z_s(s)/Z_l(s)$ meets the requirement of Nyquist stability criterion [7].

In the above analysis for stability, it is assumed that the source is ideal voltage source and it remains stable under unloaded condition. However, the grid-connected inverters are usually current controlled. Hence above analysis is not much useful. So, the source should be represented as current source. To arrive at the equivalent current source, the same small signal voltage source is modified. The voltage across load is given by

$$V(s) = \frac{I_s(s)}{Y_l(s) + Y_S(s)} \tag{4}$$

by rearranging

$$V(s) = \frac{I_s(s)}{Y_l(s)} \frac{I_s(s)}{1 + \frac{Y_S(s)}{Y_l(s)}} \tag{5}$$

Similar to the above analysis, the current source is assumed to be stable under unloaded condition. The load is stable when connected to ideal current source. Under this condition, $I(s)$ and $1/Y_l(s)$ are stable. Under this condition, stability of $V(s)$ depends on stability of second term of Eq. (5). This again resembles the closed-loop transfer function with negative feedback. The gain is unity and the feedback factor is $Y_s(s)/Y_l(s)$. Therefore the system is stable, if, along with above conditions, it meets the Nyquist criterion. In Eq. (5) admittances are used instead of impedance, though the analysis still can be carried out in terms of the impedances. In this case, Eq. (5) becomes

$$V(s) = I_s(s).Z_l(s) \frac{1}{1 + \frac{Z_l(s)}{Z_s(s)}} \tag{6}$$

It is important to note the requirement of stability. In the voltage source model, the output impedance of source should be as low as possible (ideally zero); whereas in the current source model, the output impedance should be as high as possible (ideally infinite).

4. Grid-connected inverters

The modelling of impedance of grid-connected VSC has very important use in analysis of stability and resonance phenomena when converter is integrated into the

grid [5]. The grid-connected converter used in renewable sources is modelled as a current source in parallel with an impedance, i.e. Norton's equivalent circuit [6]. The stability of grid-connected inverter can be determined by Nyquist criterion [8]. The control structure of most of the VSCs is developed in the rotating dq reference frame [7]. The phase lock loop is used to synchronise converter with grid [9]. The use of complex multiple-loop control structure introduces non-linearities. These are generally overlooked in the simplified low-order modelling [10]. On the flip side, the detailed model introduces complexity and cross-couplings between various terms, which makes the determination of output impedance cumbersome. The trade-off way suggested in some literatures is to linearise the model by small signal analysis technique.

The impedance of converter-interconnected generator is affected by various factors such as control parameters, PLL, switching delays and converter harmonic filters. The converter is basically controlled by output current signal. In **Figure 4**, i_1 is the converter current and i_2 is the grid current. The converter is controlled either by i_1 or i_2. If the grid current is the control variable, then the current control loop is

$$Y_o(s) = G_{PI}(s)G_D(s)Y_{21}(s) \tag{7}$$

where Y_{21} is the forward trans-admittance of the filter, $G_{PI}(s)$ is the proportional-integral-type current controller and $G_D(s)$ is the switching delay. Here, the converter output voltage is considered as pure sinusoidal; if there is a noise in the voltage, then it needs to be considered as a disturbance signal. If, the converter is controlled by taking converter current i_1, then Y_{21} is replaced by output conductance Y_{11}. The forward transconductance Y_{21} is given by

$$Y_{21}(s) = \frac{Z_{3f}}{Z_{1f}Z_2 + Z_{1f}Z_{3f} + Z_2Z_{3f}} \tag{8}$$

The simple transfer function of current controller is given by

$$G_{PI}(s) = k_p + \frac{k_i}{s} \tag{9}$$

Higher-order controller also can be used for current control, but here simple ***PI*** controller is considered for the sake of simplicity. The delay, estimated by Pade's approximation technique, is given by

$$G_D(s) = \frac{1}{1 + 1.5T_d s} \tag{10}$$

The frequency response of output impedance is plotted here with the line impedance. The phase at the intersection of two curves gives the phase margin (PM).

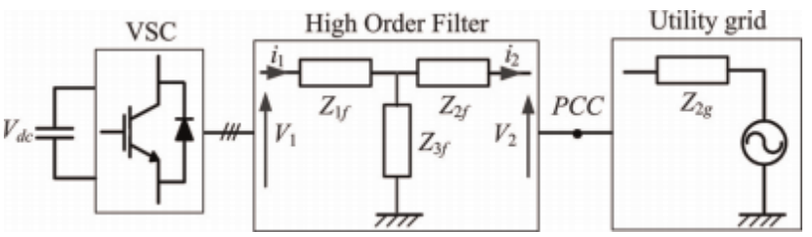

Figure 4.
Converter output circuit (Source: [11]).

5. Phase lock loop

$$G_{PLL}(s) = f(s, w, k) \tag{11}$$

The phase lock loop is required for PI-based controller. So, the structure of PLL should be thoroughly assessed for stability. Proper structure of PLL and control scheme helps to mitigate adverse impact on the system. The purpose of PLL is to synchronise converter with grid. Harmonics in the grid may penetrate to the converter through the PI controller. If control parameters are not properly chosen, this may produce harmonics through circular effect. **Figure 5** shows the block diagram of PLL. The detail block diagram is given in **Figure 6**.

Figure 6 is the traditional second-order generalised integrator–quadrature signal generator (SOGI-QSG) PLL. It can filter out higher-order harmonics, where u_i is the input signal; u_i' and qu_i' are two output signals, which are in quadrature; k is the damping coefficient; and ω' is the output angular frequency of PLL. Eqs. (14) and (15) show the transfer function of PLL.

$$G_1(s) = \frac{u_i'}{u_i} \tag{12}$$

$$G_1(s) = \frac{u_i'}{u_i} = \left[(u_i - u_i')k - u_i'\omega'/s\right] * \omega'/s = u_i' \tag{13}$$

Simplifying above equation gives

$$G_1(s) = \frac{u_i'}{u_i} = \frac{k\omega' s}{s^2 + k\omega' s + \omega'^2} \tag{14}$$

Similarly, for quadrature output transfer function is

$$H_1(s) = \frac{qu_i'}{u_i} = \frac{k\omega'^2}{s^2 + k\omega' s + \omega'^2} \tag{15}$$

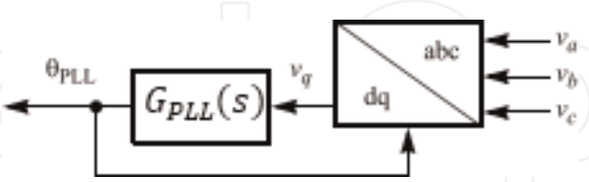

Figure 5.
Phase lock loop.

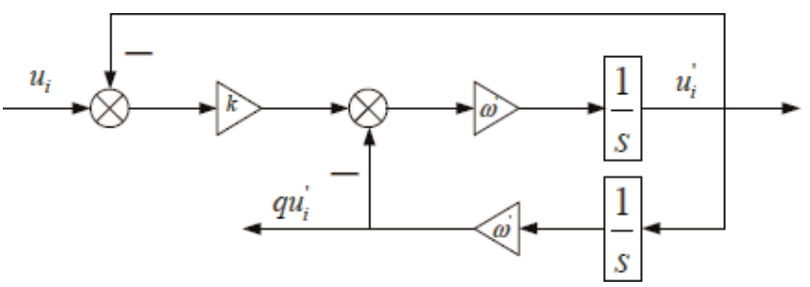

Figure 6.
Block diagram of simple phase lock loop.

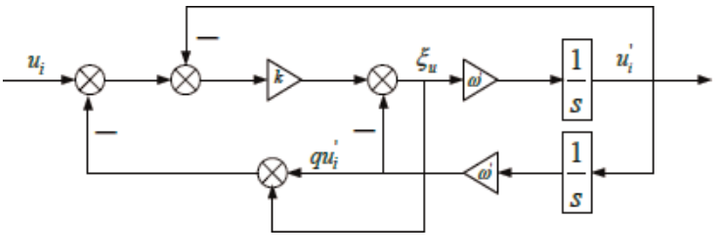

Figure 7.
Block diagram of modified phase lock loop.

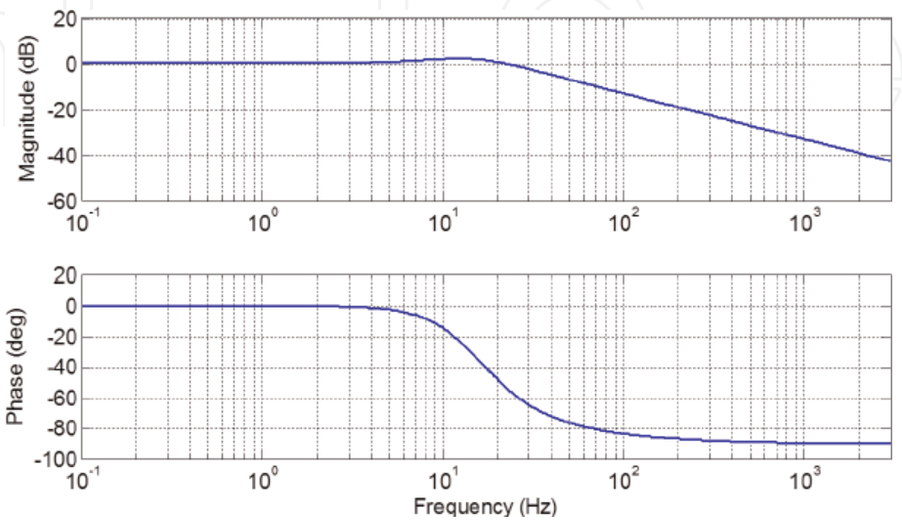

Figure 8.
Frequency response of simple phase lock loop.

In traditional SOGI-QSG PLL, the DC component in the input signal is not suppressed by the PLL. To overcome this problem, a minor modification is made in above PLL. The modified PLL is shown in **Figure 7**.

Transfer functions of modified PLL are given in Eqs. (16)–(18). This structure reduces the tracking error of PLL.

$$F_2(s) = \frac{\xi_u}{u_i} = \frac{ks^2}{s^2 + k\omega' s + \omega'^2} \tag{16}$$

$$G_2(s) = \frac{u_i'}{u_i} = \frac{k\omega' s}{(k+1)s^2 + k\omega' s + (k+1)\omega'^2} \tag{17}$$

$$H_2(s) = \frac{qu_i'}{u_i} = \frac{k\omega'^2}{(k+1)s^2 + k\omega' s + (k+1)\omega'^2} \tag{18}$$

The bode plot of one of the PLL used in [12] is given here. The bandwidth of the PLL is 33 Hz. It attenuates harmonics of 1 kHz to −30 dB. However, the effect of PLL with other controllers and output filter needs to be investigated for crucial stability analysis (**Figure 8**).

6. Damped passive filter topologies

Different types of passive filters are used in converter-based renewable generation sources. The effectiveness of filter, particularly passive type, primarily depends on the grid strength and variation of grid impedance with time. LCL is the common type of filter used widely. The variation in grid impedance affects the performance

of LCL filter. Hence, the design of LCL filter is a trade-off between robustness and damping of resonance. The effective impedance with simple PI controller is explained here with RL filter topology.

6.1 R-L filter

Applying KVL at the converter output gives

$$V_c - V_{POC} = I_{fg}\left(R_{fc} + SL_{fc}\right) \tag{19}$$

Converter output is controlled by output current

$$V_c = f\left(I_{fg}\right) \tag{20}$$

With simple PI controller, the output becomes

$$V_c = \left(k_P + \frac{k_i}{s}\right)\left(I_{fg}\right) \tag{21}$$

Putting Eq. (20) into Eq. (18)

$$\left(k_P + \frac{k_i}{s}\right)\left(I_{fg}\right) - V_{POC} = I_{fg}\left(R_{fc} + SL_{fc}\right) \tag{22}$$

$$\left(\left(k_P + \frac{k_i}{s}\right)I_{fg}\right) - I_{fg}\left(R_{fc} + SL_{fc}\right) = V_{POC} \tag{23}$$

$$Z_o = \frac{\left(S^2 L_{fc} + S\left(R_{fc} - k_p\right) - k_i\right)}{S} \tag{24}$$

$$Z_o = \frac{(S+\alpha)(S+\beta)}{S} \ (considering\ \alpha < \beta) \tag{25}$$

Equation (25) shows that there are two zeros and one pole. First, the output impedance decreases at −20 dB per decade up to first zero at α. At α, the impedance response becomes flat, and at β the impedance starts increasing at 20 dB per decade (**Figure 9**). So, the response of integrated filter becomes similar to that of series resonance filter. The selection of α and β depends on the parameter selection of L_{fc}, R_{fc}, k_P and k_i. Bode plot for RL filter without and with PI current controller is given in **Figures 10** and **11**, respectively.

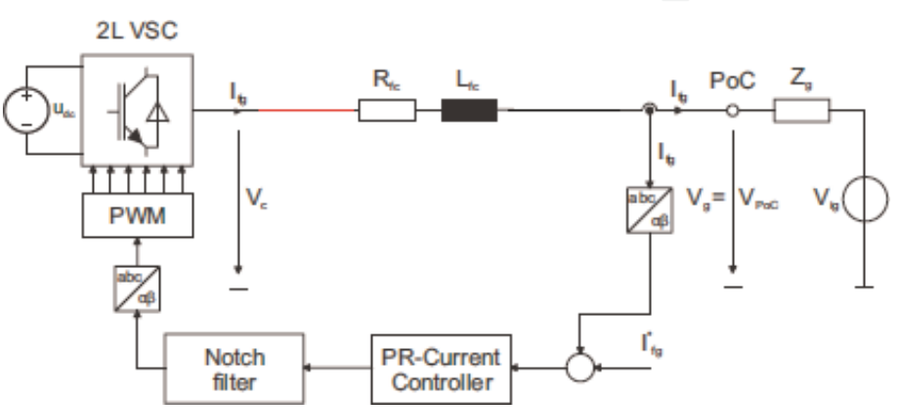

Figure 9.
Grid-connected inverter with filter.

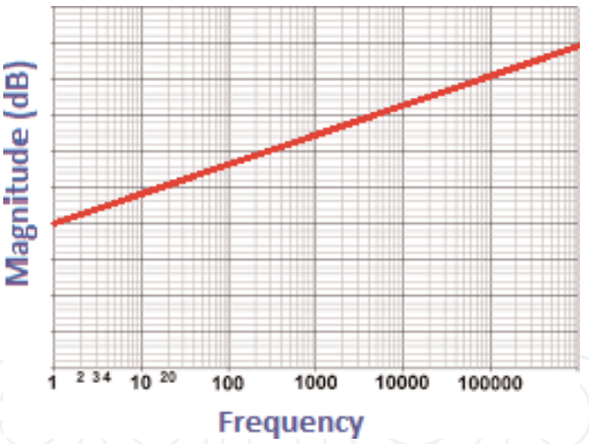

Figure 10.
Frequency response of impedance with RL filter without PI controller.

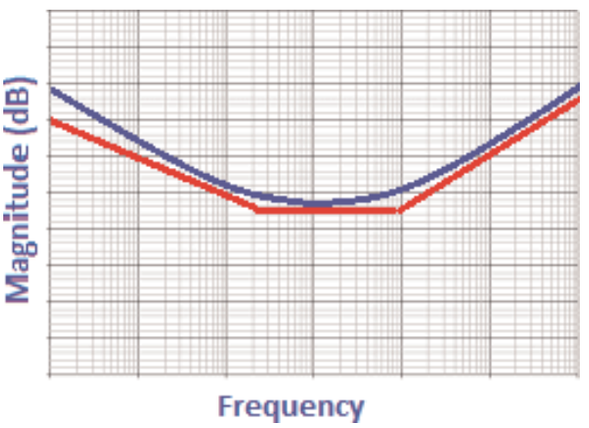

Figure 11.
Frequency response of impedance with RL filter with PI controller.

6.2 L-C filter

LC filter is used in converters for industrial applications like variable frequency drive (VFD) and uninterrupted power supply (UPS). It is simple in construction and relatively less costly. The analysis of LC filter with PI controller is given here (**Figure 12**).

As per the standard practice, the value of L is selected such that its impedance at fundamental frequency should not drop by more than 3% of rated voltage. The capacitive reactance offers 1/5th of the fundamental inductive reactance at switching frequency of converter (around 3–4 kHz) to absorb harmonics effectively. Based on these criteria, LC filter is widely designed. The frequency response of LC filter with and without PI controller is given in **Figures 13** and **14**,

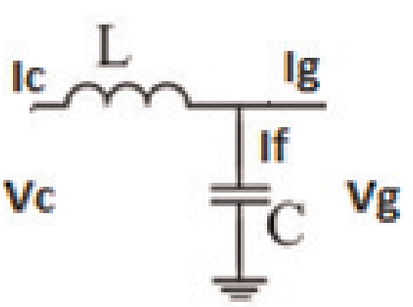

Figure 12.
L-C filter.

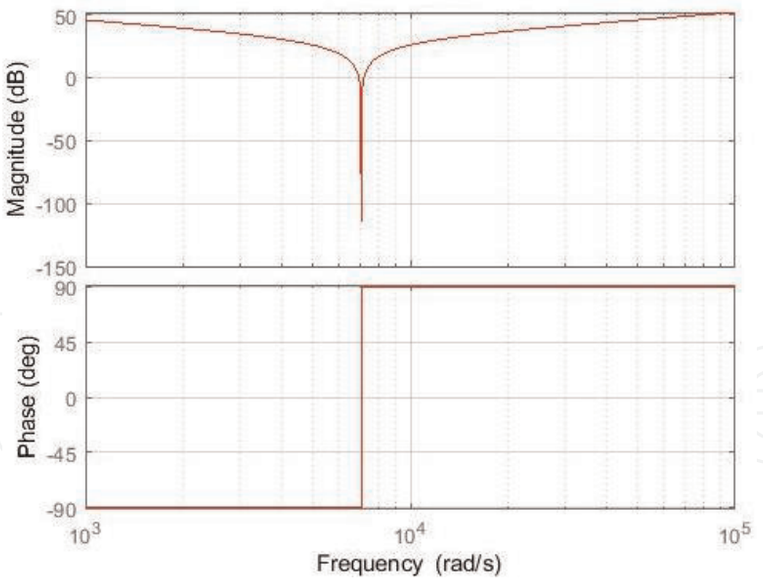

Figure 13.
Frequency response of LC filter without PI controller.

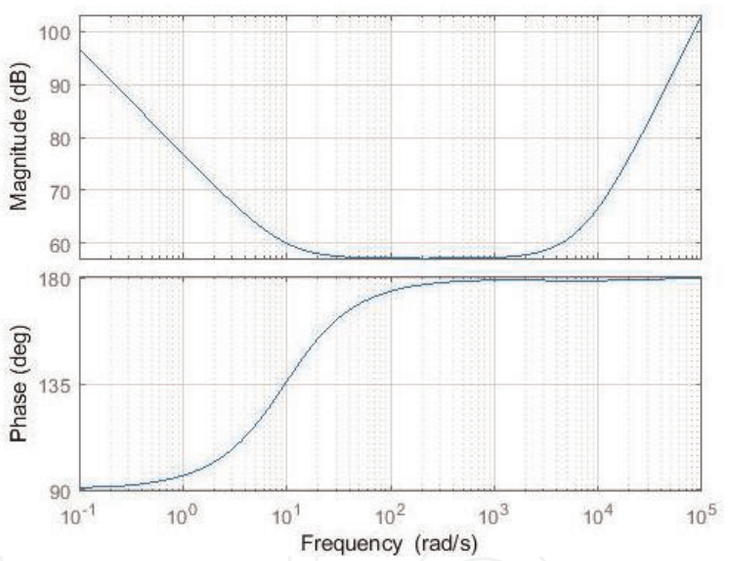

Figure 14.
Frequency response of LC filter with PI controller.

respectively. It is clear from the difference in bode plot that PI controller changes the frequency response.

6.3 L-C-L filter

Initially LC filter was used for converter applications, but grid-connected inverter has unique requirements that LC filter may not provide. Properly designed LCL filter may overcome the drawbacks of LC filter (**Figure 15**).

Applying KVL,

$$V_c = \left(\frac{(V_g + L_g s I_g)}{\frac{1}{sC_f} + R} + I_g \right) sL_c \tag{26}$$

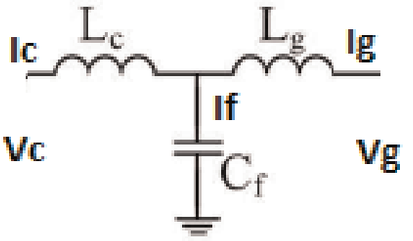

Figure 15.
L-C-L filter.

The converter output voltage V_c is a function of the grid current I_g. Then

$$V_c = f(I_g) \tag{27}$$

$$V_c = \left(k_p + \frac{k_i}{s}\right) I_g \tag{28}$$

Putting this in Eq. (26) and simplifying further give

$$Z_0 = \frac{V_g}{(-I_g)} = \frac{a_4 s^4 + a_3 s^3 + a_2 s^2 + a_1 s^1 + a_0}{b_3 s^3 + b_2 s^2 + b_1 s^1 + b_0} \tag{29}$$

where

$$a_4 = L_g C_f k_p$$

$$a_3 = L_g C_f k_i + R C_f L_g k_p$$

$$a_2 = R L_g C_f k_i + L_c k_p - C_f$$

$$a_1 = L_c k_i$$

$$a_0 = 0$$

$$b_3 = L_c C_f k_p$$

$$b_2 = L_c C_f k_i$$

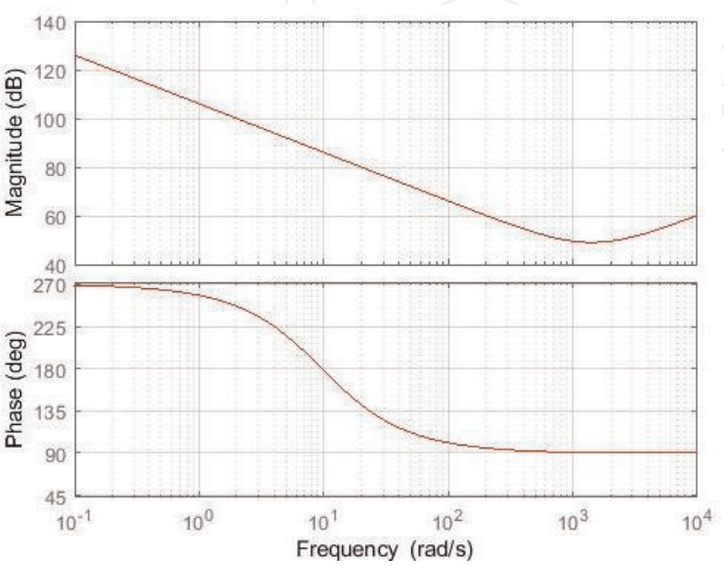

Figure 16.
Frequency response of LCL filter with PI controller.

$$b_1 = 0$$

$$b_0 = 0$$

Figure 16 shows the frequency response of LCL filter together with PI controller. It is clear from Eq. (29) and from **Figure 16** that the PI controller increases the order of filter, so the frequency response of passive filter gets changed by the controller action.

7. Optimised filter design

The design criterion for filter design should comply with the regulatory requirement. As per IEEE 519-1992 standard, the current harmonics for weak grid condition (I_{sc}/I_L) should be less than 0.3%. The ripple is caused by pulse width modulated signal. Output voltage varies from zero level to DC voltage level (V_{dc}). The modulated wave causes ripple in the current, which can be reduced by proper selection of output filter parameters. Typical L-C-L filter is used in most of the inverter. The L1-C-L2 filter has three unknowns. The selection of these parameters depends on various factors. Grid condition is one of them. The strength of the grid decides the effectiveness of filters. Typical grid impedance varies from 5 to 8% with X/R ratio in the range of 7–10 [13].

The switching frequency decides the ripple level and ripple frequency. Generally, inverter switching frequency remains in the range of 3–5 kHz. The ripple current is reduced either by increasing switching frequency or by using passive filter at the inverter/converter output. Higher switching frequency is selected to reduce the ripple current at the generation point, but it adversely affects the converter (IGBT) losses [14]. The second option is to use large inductor at the output of converter, but this not only incurs high cost but also increases the core losses. Typically 20% ripple current is expected in the output current. Keeping this in consideration, the inductor L1 is given by [7]

$$L_1 = \frac{1}{8} x \frac{V_{dc}}{\Delta I_L f_{sw}} = \frac{1}{8} x \frac{V_{dc}}{0.2\, I_{rated} f_{sw}} \tag{30}$$

The capacitor rating is selected such that the reactive power of capacitor is neither too high nor too low. Higher reactive power demands more power from converter, which causes more loss in reactor L1 and also more loss in converter switches. A lower value of capacitor will increase the inductor size. So, the capacitor is selected so that the reactive power should be in the range of 15–20% of the rated power.

$$C = 0.15x \frac{P_r}{\omega\, V_r^2} \tag{31}$$

7.1 Passive damping of filter

7.1.1 Type I filter

In LCL filter, the damping can be achieved by simply adding series resistance in series with capacitor C. It is obvious that large value of damping resistance (Rd) gives large damping. But damping is effective around the resonance point only [15]. Above the resonance point, damping weakens. Also, the large value of resistance causes higher losses (**Figure 17**).

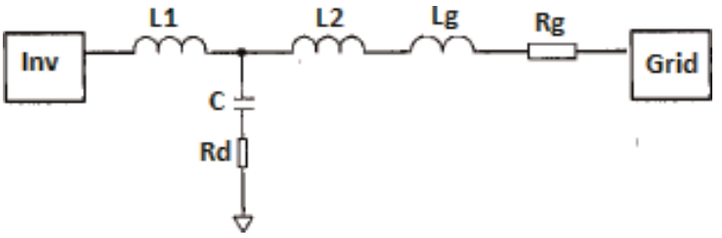

Figure 17.
Type I LCL filter.

Impedance of Type I LCL filter with damping resistance is given by

$$Z_o = \frac{a_4 s^4 + a_3 s^3 + a_2 s^2 + a_1 s^1 + a_0 s^0}{b_2 s^2 + b_1 s^1 + b_0 s^0} \tag{32}$$

where

$$a_4 = L_g L_1 C^2$$
$$a_3 = L_1 C^2 (R_d + R_g)$$
$$a_2 = L_g R_d C + L_1 C$$
$$a_1 = L_g + C R_d R_g$$
$$a_0 = R_g$$
$$b_2 = L_g C$$
$$b_1 = (R_g + R_d) C$$
$$b_0 = 1$$

Frequency response of LCL filter with damping resistor is given in **Figure 18**. The grid parameters are Lg = 0.212 mH and Rg = 0.0095 Ohm, whereas the filter parameters are L_1 = 0.450 mH, L_2 = 0.300 mH and C = 270 uF. The damping resistance is varied from 0.05 to 0.8 Ohm. It is clear from the plot that the response of impedance is similar to inductive impedance. The notch is observed at the resonant frequency, which can be dampened by resistor in series with capacitor.

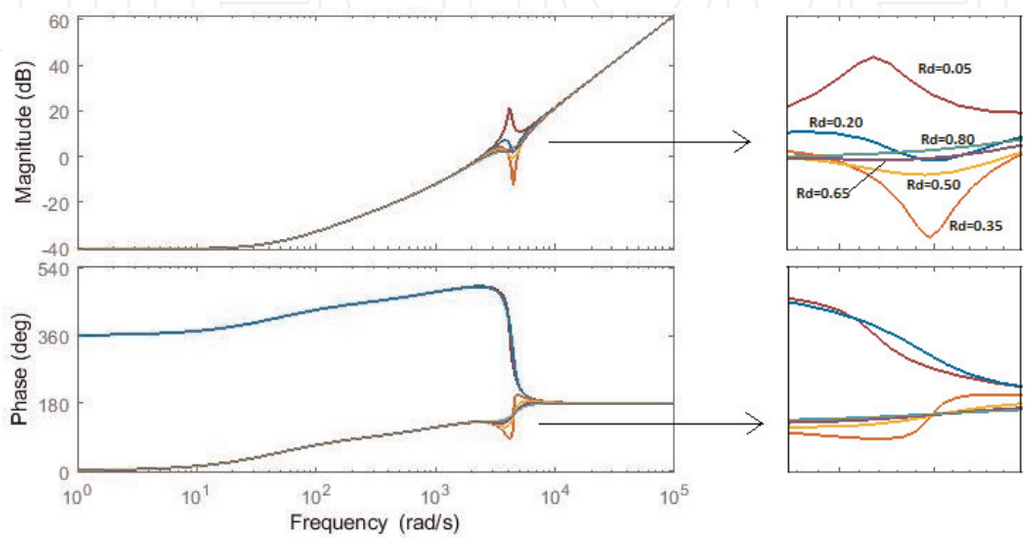

Figure 18.
Nyquist plot of Type I LCL filter.

The gain margin is −40 dB and phase margin is around 120°. So, as per the Nyquist criterion, the filter response is very stable.

7.1.2 Type II filter

In Type II LCL filter (**Figure 19**), the damping can be achieved by simply adding a parallel combination of resistor and inductor in series with capacitor C. The effect of inductor is investigated using Nyquist plot. The value of R_f = 10 Ohm and L_f is varied from 50 to 500 μH. The effect of increase in L_f observed using Nyquist plot is given in **Figure 20**.

Impedance of Type II LCL filter with damping inductor and resistance is given by

$$Z_o = \frac{a_4 s^4 + a_3 s^3 + a_2 s^2 + a_1 s^1 + a_0 s^0}{b_3 s^3 + b_2 s^2 + b_1 s^1 + b_0 s^0} \tag{33}$$

where

$$a_4 = CL_1L_f\left(L_g + L_2\right)$$
$$a_3 = L_1CL_fR_f + CL_1L_fR_g + CR_f\left(L_2 + L_g\right) + CR_fL_f\left(L_2 + L_g\right)$$
$$a_2 = L_1L_f + CL_1R_fR_g + CL_fR_fR_g + L_f\left(L_2 + L_g\right)$$
$$a_1 = L_1R_f + L_fR_g + R_f\left(L_2 + L_g\right)$$
$$a_0 = R_fR_g$$

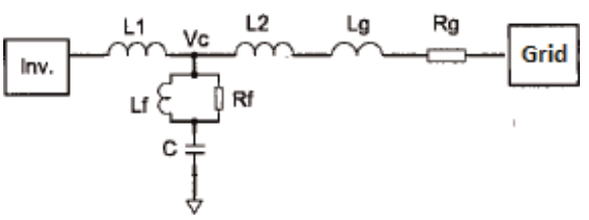

Figure 19.
Type II LCL filter.

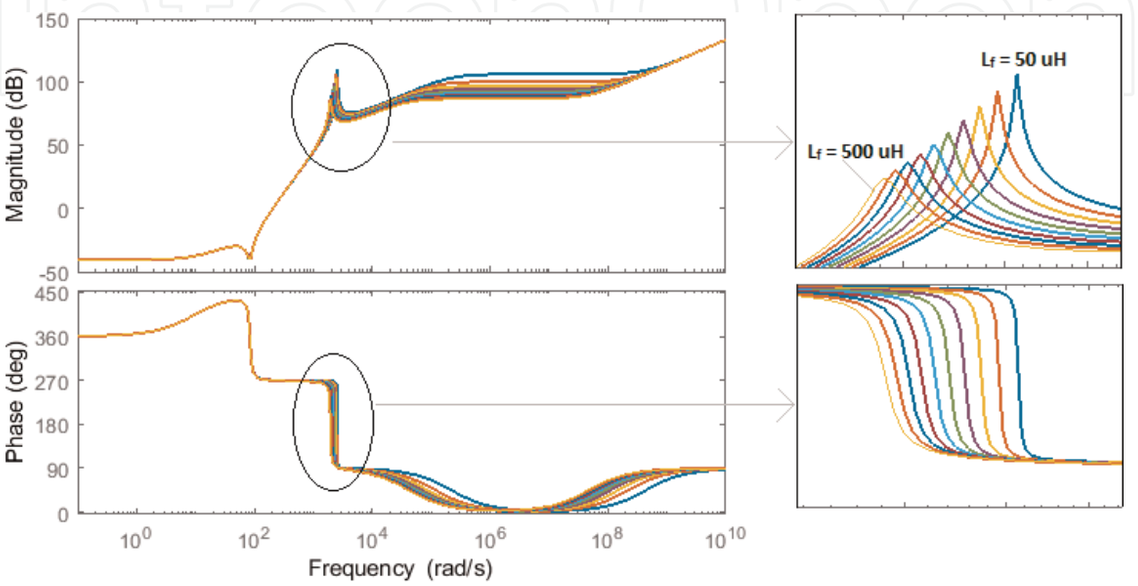

Figure 20.
Nyquist plot of Type II LCL filter.

$$b_3 = CL_f\left(L_2 + L_g\right)$$
$$b_2 = CL_fR_f + CL_fR_g + CR_f\left(L_2 + L_g\right)$$
$$b_1 = L_f + CR_fR_g$$
$$b_0 = R_f$$

From the bode graph, it is observed that the gain margin is 70–100 dB for various values of L_f. Similarly, the phase margin is 270°. As the value of L_f is increased, there will be reduction in the gain margin.

7.1.3 Type III filter

In Type III LCL filter, the damping can be achieved by simply adding a parallel combination of resistor and inductor in series with capacitor C. The effect of inductor is investigated using Nyquist plot (**Figure 21**).

Impedance of Type III LCL filter with damping inductor and resistance is given by

$$Z_o = \frac{a_4s^4 + a_3s^3 + a_2s^2 + a_1s^1 + a_0s^0}{b_3s^3 + b_2s^2 + b_1s^1 + b_0s^0} \tag{34}$$

where

$$a_4 = CC_fL_1\left(L_g + L_2\right) + CL_1L_fC_f$$
$$a_3 = L_1CC_fR_g + CL_1C_fR_f + C_fL_f\left(L_2 + L_g\right)$$
$$a_2 = L_1C + C_f\left(L_2 + L_g\right)R_f + C_fL_fR_g$$
$$a_1 = L_1C_f + C_fR_gR_f + \left(L_2 + L_g\right)$$
$$a_0 = R_g$$
$$b_3 = CC_f\left(L_2 + L_g\right) + CL_fC_f$$
$$b_2 = CC_fR_g + CC_fR_f$$
$$b_1 = C_f$$
$$b_0 = 0$$

Impedance shows two resonance points: first is parallel resonance and second is series resonance (**Figure 22**). At first resonance point, the output impedance increases, and at series resistance it is at the minimum value. The phase margin of filter is around 210°. This ensures the stability of filter. The resonant frequency will shift with change in grid resistance, so the damping effect is difficult to predict.

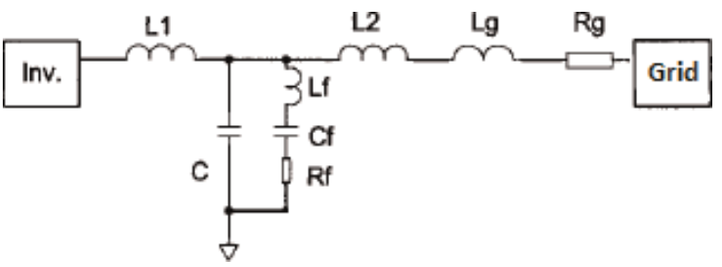

Figure 21.
Type III LCL filter.

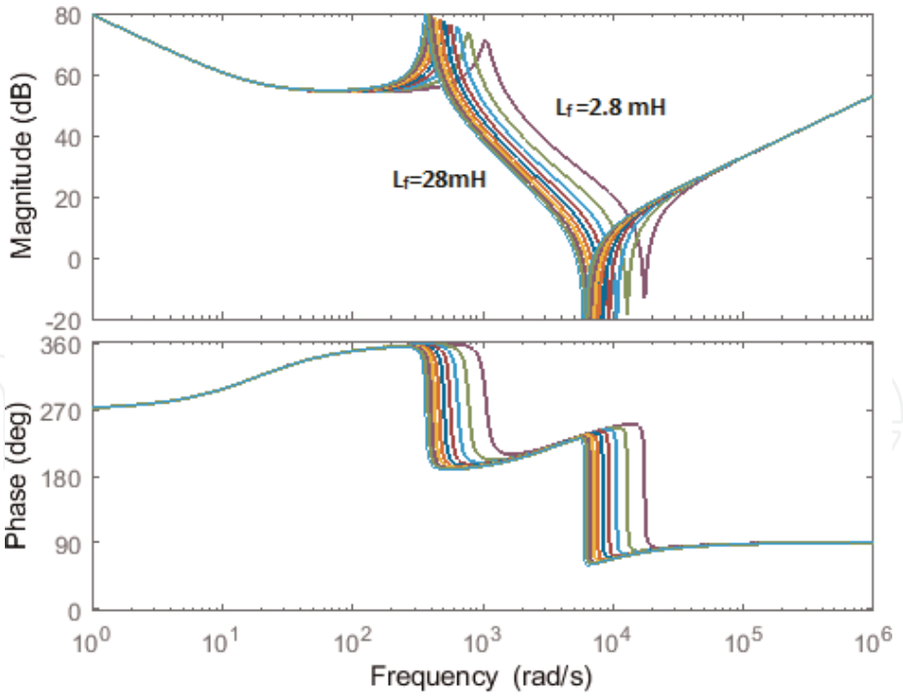

Figure 22.
Nyquist plot of Type III LCL filter.

7.1.4 Type IV filter

In Type IV LCL filter, the damping can be achieved by simply adding a parallel combination of resistor and capacitor Cf. The effect of resistor value is investigated using Nyquist plot (**Figure 23**).

Impedance of Type IV LCL filter with damping resistor R_f in series with capacitor C_f is given by

$$Z_o = \frac{a_4 s^4 + a_3 s^3 + a_2 s^2 + a_1 s^1 + a_0 s^0}{b_3 s^3 + b_2 s^2 + b_1 s^1 + b_0 s^0} \tag{35}$$

where

$$a_4 = CC_f L_1 (L_g + L_2)$$
$$a_3 = CC_f L_1 R_f + CC_f R_g L_1$$
$$a_2 = L_1 C_f + L_1 C + C_f R_f (L_2 + L_g) + C_f (L_2 + L_g)$$
$$a_1 = C_f R_f R_g$$
$$a_0 = R_g$$
$$b_3 = CC_f (L_2 + L_g)$$

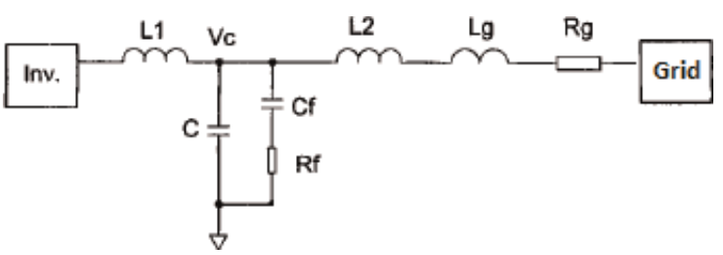

Figure 23.
Type IV LCL filter.

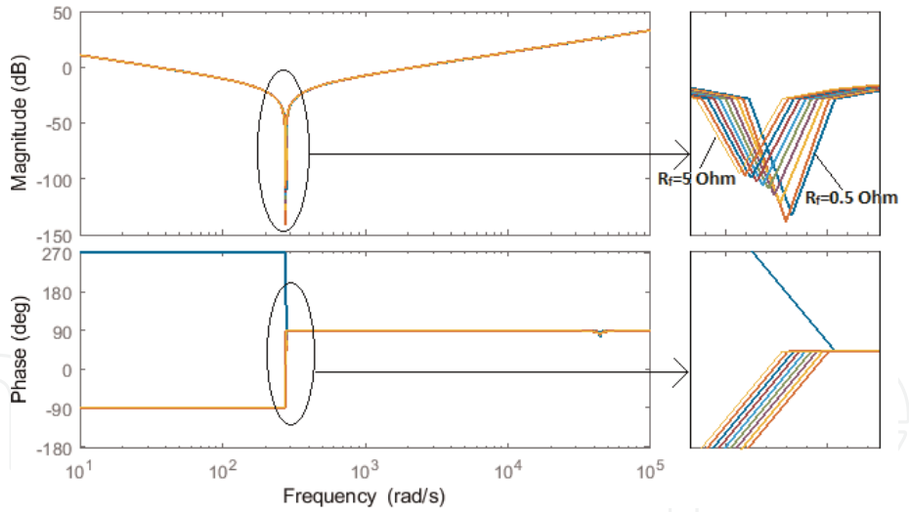

Figure 24.
Nyquist plot of Type IV LCL filter.

$$b_2 = CC_f R_g + CC_f R_f$$
$$b_1 = C_f + C$$
$$b_0 = 0$$

The response of Type IV filter is similar to the tuned filter. The notch in frequency response of impedance is observed at the resonant frequency (**Figure 24**). This notch can be damped by putting higher value of resistor in series with the capacitor C_f. The phase of impedance sharply changes from −90 to 90°, which means the nature of impedance turns from capacitive to inductive. The ratio of C_f/C decides the damping effectiveness. The larger the C_f/C ratio, the larger will be the damping. Also, with increasing value of C_f/C ratio, the loss in resistor R_f is also increases as more and more current tends to flow in it [16–18].

7.1.5 Type V filter

In Type V LCL filter, the damping can be achieved by simply adding a parallel combination of resistor and inductor with capacitor C. The effect of inductor is investigated using Nyquist plot (**Figure 25**).

Impedance of Type V LCL filter is given by

$$Z_o = \frac{a_5 s^5 + a_4 s^4 + a_3 s^3 + a_2 s^2 + a_1 s^1 + a_0 s^0}{b_4 s^4 + b_3 s^3 + b_2 s^2 + b_1 s^1 + b_0 s^0} \tag{36}$$

where

$$a_5 = CC_f L_1 L_f (L_g + L_2)$$
$$a_4 = CC_f L_1 L_f R_f + CC_f L_1 R_f (L_g + L_2) + CC_f L_1 L_f R_g$$
$$a_3 = CL_f L_1 + CC_f L_1 R_f + C_f L_f R_f (L_g + L_2)$$
$$a_2 = L_1 CR_f + L_f (L_2 + L_g) + L_f C_f R_f R_g$$
$$a_1 = L_1 + R_f (L_2 + L_g) + L_f R_g$$
$$a_0 = R_f R_g$$

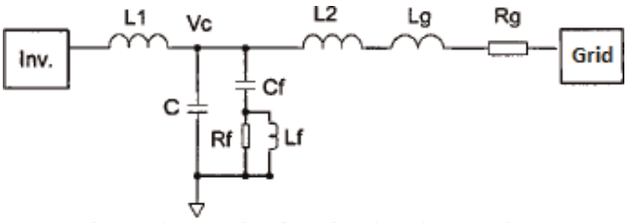

Figure 25.
Type V LCL filter.

$$b_4 = L_f C C_f (L_2 + L_g)$$
$$b_3 = L_f C C_f R_f + L_f C C_f R_g + C_f R_f (L_g + L_2)$$
$$b_2 = L_f C + C C_f R_f$$
$$b_1 = R_f C$$
$$b_0 = 1$$

Type V filter response shows two resonance frequency (**Figure 26**). The first resonance creates high voltage distortion, while the second resonance point gives rise to current distortion. If converter generates harmonics equal to this resonance, then there will be high voltage distortion and current distortion. However, with lower value of resistance, damping can be achieved. An additional inductor L_f can reduce the resistive loss.

7.2 Active damping of filter

Grid-connected converters may not function stably under the harmonic resonance condition. Harmonic resonance occurs when the converter impedance and grid impedance becomes equal in magnitude and 180° out of phase. The converter is generally connected to grid through filters, which is mostly LCL type. So, the parameters of LCL filters play an important role in keeping the successful functioning of converter. Also, the control structure of the converter shapes its output impedance. So, the control parameter should be selected such that it keeps the converter in the safe zone at all frequency. This is explained further here with analysis.

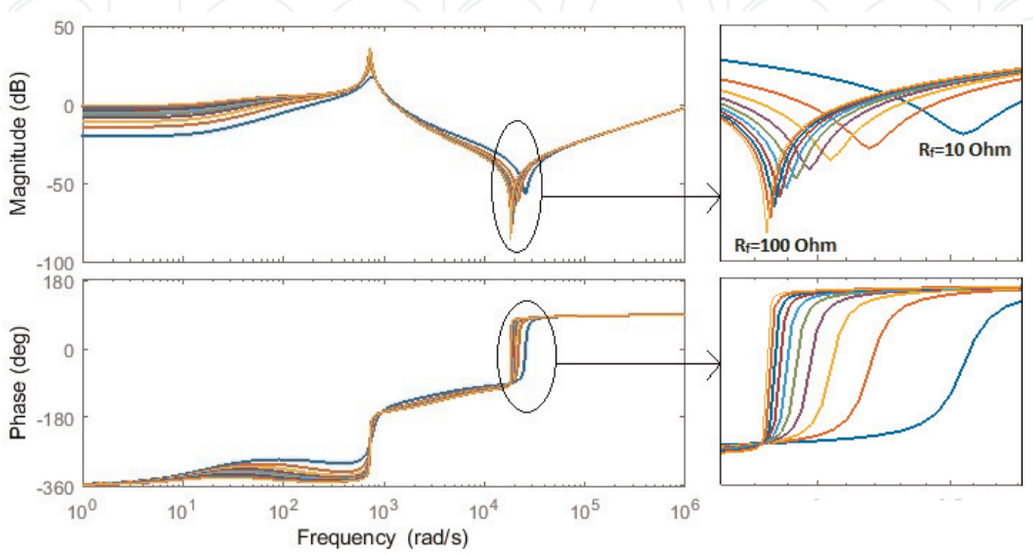

Figure 26.
Nyquist plot of Type V LCL filter.

The inverter output characteristics depend on several factors like parameter of LCL filter, grid impedance, type of controller and control parameters. By selecting the appropriate parameter, the inverter can be operated with resistive output impedance, inductive output impedance and capacitive output impedance. Most of the inverters are operated with inductive (L-type) output impedance. This inverter is known as the L-type inverter. Here it is explained how an inverter impedance can be made capacitive (C-type inverter) with selection of virtual current control loop.

The output impedance of inverter is controlled by the virtual impedance. The single-line diagram of inverter with control loop is shown in **Figures 27** and **28**. The control is implemented with current loop and voltage loop, which gives good tracking behaviour and good output voltage. The feedback of current is taken from branch between the two capacitors. The first capacitor has a value of βC, and the second capacitor has a value of (1-β)C. Thus, the overall value of capacitor is C. The output impedance of system after adding virtual branch G_V is given by

$$Z_o = \frac{(G_I + G_V)K_{PWM} + L_s + r}{Cs(L_s + r) + Cs(1-\beta)K_{PWM}(G_I + G_V) + G_I G_U K_{PWM} + 1} \tag{37}$$

The value of virtual impedance G_V decides the overall impedance characteristics of output impedance. If G_V is selected as per Eq. (38),

$$G_V + G_I = \frac{G_I G_U K_{PWM} + 1}{Cs\beta K_{PWM}} \tag{38}$$

$$Z_0 \approx \frac{1}{Cs} \tag{39}$$

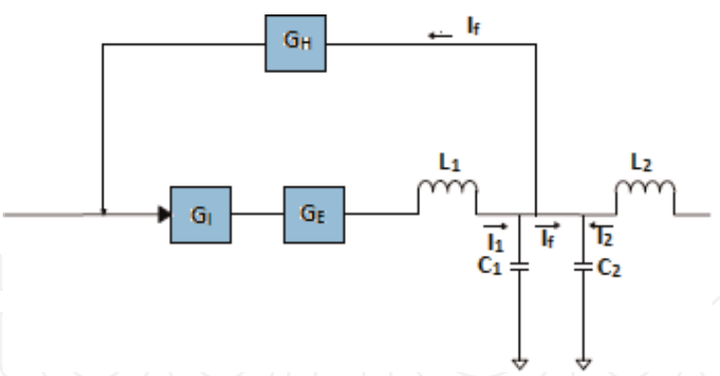

Figure 27.
Block diagram for active damping.

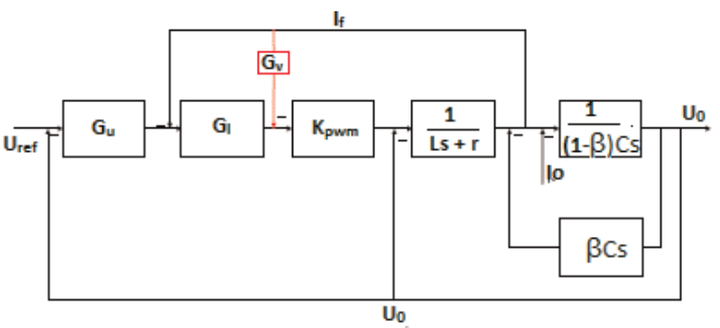

Figure 28.
Control diagram of active damping of filter.

With the above value of G_V, the output impedance becomes capacitive. So, by selection of proper control loop and control parameter, the shaping of inverter output impedance can be effectively done. Also, the desired value of damping can be achieved. This method is known as active damping method. Like this, the inverter can be made either L-type or R-type.

8. Conclusion

The characteristics and response of impedance of grid-connected inverter depend on various factors like selection of output filter and its parameter, controller type and its parameters, structure of PLL, the delay in switching of converter, etc. In this chapter, using first-order PI controller and different controller types, it is explained in a simple way. The complexity of impedance increases with the order of the controller and its structure. Also, the reshaping of inverter impedance can be done by selection of suitable control structure. By adding virtual impedance, the output impedance can be made inductive, capacitive or reactive without adding any additional hardware. In this work different variants of passive filter are explained, and how their output impedance behaves at different frequency is also explained with the use of Nyquist plot. The active damping method is explained, whereby damping is achieved without using resistor in the filter, which is considered as a very energy-efficient method of achieving damping. The output impedance can be reshaped either by external hardware in the form of filter or by adding virtual control loop in the controller. The stability of converter depends on how converter output impedance interacts with the grid impedance. Numerous efforts have been made and can be found in literatures to achieve the stability only by reshaping the impedance. However, the stability region can be expanded by reshaping of impedance up to a certain extent only. Only reshaping of impedance does not guarantee the converter stability with changing grid condition. Also, the converter is more likely to fall in an unstable region with weak grid condition, but reshaping of impedance helps to prevent converter-based generation from going unstable. By analysing the output impedance in the frequency domain, the controller parameters can be adjusted to reshape the output impedance. By increasing the proportional gain of the PI controller, the magnitude of the output impedance can be increased and can enhance the ability of harmonic rejection. By increasing the integral gain of the PI controller, the phase of the output impedance can be increased to improve the stability of the system [19, 20] (**Table 1**).

Switching frequency	4 kHz
Switching delay	20 μS
Lc	4 mH
Lg	0.4 mH
Cf	5 μF
kp	1.2
ki	11.6

Table 1.
Converter parameter.

DOI: http://dx.doi.org/10.5772/intechopen.89167

Author details

Jignesh Pravinbhai Patel and Satish Kantilal Joshi*
Department of Electrical Engineering, The Maharaja Sayajirao University of Baroda, Vadodara, Gujarat, India

*Address all correspondence to: skjoshi@ieee.org

References

[1] Blaabjerg F, Zhe C, Kjaer SB. Power electronics as efficient interface in dispersed power generation systems. IEEE Transactions on Power Electronics. 2004;**19**(5):1184-1194

[2] Ali MH, Wu B, Dougal RA. An overview of SMES applications in power and energy systems. IEEE Transactions on Sustainable Energy. 2010;**1**(1):38-47

[3] Flourentzou N, Agelidis VG, Demetriades GD. VSC-based HVDC power transmission systems: An overview. IEEE Transactions on Power Electronics. 2009;**24**(3):592-602

[4] Xia J, Fang X, Chow JH, Edris A, Uzunovic E, Parisi M, et al. A novel approach for modeling voltage-sourced converter-based FACTS controllers. IEEE Transactions on Power Delivery. 2008;**23**(4):2591-2598

[5] He J, Li YW. Generalized closed-loop control schemes with embedded virtual impedances for voltage source converters with LC or LCL filters. IEEE Transactions on Power Electronics. 2012;**27**(4):1850-1861

[6] Sun J. Impedance-based stability criterion for grid-connected inverters. IEEE Transactions on Power Electronics. 2011;**26**(11):3075-3078

[7] Blaabjerg F, Teodorescu R, Liserre M, Timbus AV. Overview of control and grid synchronization for distributed power generation systems. IEEE Transactions on Industrial Electronics. 2006;**53**(5):1398-1409

[8] Middlebrook RD. Input filter considerations in design and application of switching regulators. In: Proceedings of the IEEE-IAS Annual Meeting; 1976. pp. 366-382

[9] Freijedo FD, Yepes AG, Lopez O, Vidal A, Doval-Gandoy J. Three-phase PLLs with fast postfault retracking and steady-state rejection of voltage unbalance and harmonics by means of lead compensation. IEEE Transactions on Power Electronics. 2011;**26**(1):85-97

[10] Wang F, Duarte JL, Hendrix MAM, Ribeiro PF. Modeling and analysis of grid harmonic distortion impact of aggregated DG inverters. IEEE Transactions on Power Electronics. 2011;**26**(3):786-797

[11] Beres RN, Wang X, Blaabjerg F, Liserre M, Bak CL. Optimal design of high-order passive-damped filters for grid-connected applications. IEEE Transactions on Power Electronics. 2016. DOI: 10.1109/TPEL.2015.2441299

[12] Sun J. Small-signal methods for AC distributed power systems—A review. IEEE Transactions on Power Electronics. 2009;**24**(11):2545-2554

[13] Li X-Q, Wu X-J, Geng Y-W, Zhang Q. Stability analysis of grid-connected inverters with an LCL filter considering grid impedance. Journal of Power Electronics. 2013;**13**(5)

[14] Jiao J, Nelms RM. Regulating output impedance using a PI controller to improve the stability of a single phase inverter under weak grid. In: 2016 IEEE 16th International Conference on Environment and Electrical Engineering (EEEIC); 2016

[15] Yang W, Wang M. Impedance modeling and output impedance coupling analysis of three-phase grid-connected inverters. In: 2018 IEEE International Power Electronics and Application Conference and Exposition (PEAC); 2018

[16] Zhong Q-C, Zeng Y. Control of inverters via a virtual capacitor to achieve capacitive output impedance.

IEEE Transactions on Power Electronics;**29**(10):5568-5578. DOI: 10.1109/tpel.2013.2294425

[17] He Y, Lai C-t, Chung S-h, Zhang X, Wu W. Use of series negative impedance to cancel the effect of equivalent grid impedance on the grid connected inverter in the DPGS. In: 2018 IEEE Applied Power Electronics Conference and Exposition (APEC); 2018

[18] Zhong Q-C, Zeng Y. Universal droop control of inverters with different types of output impedance. IEEE Open Access. 2016. DOI: 10.1109/ACCESS.2016.2526616

[19] Messo T, Luhtala R, Aapro A, Roinila T. Accurate impedance model of grid connected inverter for small signal stability assessment in high-impedance grid. In: 2018 International Power Electronics Conference (IPEC-Niigata 2018 -ECCE Asia); 2018

[20] Ling P, Peng Z, Chao G. An impedance reshaping control strategy to enhance adaptability to grid for grid-connected inverters. In: 2018 China International Conference on Electricity Distribution (CICED); 2018